Analytical and Bioanalytical Chemistry
https://doi.org/10.1007/s00216-020-02608-6

RESEARCH PAPER

A high-resolution measurement of nucleotide sugars by using ion-pair reverse chromatography and tandem columns

Sha Sha[1] · Garry Handelman[2] · Cyrus Agarabi[3] · Seongkyu Yoon[1,4]

Received: 21 January 2020 / Revised: 8 March 2020 / Accepted: 18 March 2020

Abstract

N-Linked glycosylation is a cellular process transferring sugars from glycosyl donors to proteins or lipids. Biopharmaceutical products widely produced by culturing mammalian cells such as Chinese hamster ovary (CHO) cells are typically glycosylated during biosynthesis. For some biologics, the N-linked glycan is a critical quality attribute of the drugs. Nucleotide sugars are the glycan donors and impact the intracellular glycosylation process. In current analytical methods, robust separation of nucleotide sugar isomers such as UDP glucose and UDP galactose remains a challenge because of their structural similarity. In this study, we developed a strategy to resolve the separation of major nucleotide sugars including challenging isomers based on the use of ion-pair reverse phase (IP-RP) chromatography. The strategy applies core-shell columns and connects multiple columns in tandem to increase separation power and ultimately enables high-resolution detection of nucleotide sugars from cell extracts. The key parameters in the IP-RP method, including temperature, mobile phase, and flow rates, have been systematically evaluated in this work and the theoretical mechanisms of the chromatographic behavior were proposed.

Keywords Nucleotide sugars · UDP sugars · Chinese hamster ovary · Ion-pair reverse chromatography · Core-shell · Columns in tandem

Abbreviations

ADP	Adenosine diphosphate
AMP	Adenosine monophosphate
ATP	Adenosine triphosphate
CDP	Cytidine diphosphate
CMP	Cytidine monophosphate
CTP	Cytidine triphosphate
CMP-SA	Cytidine monophosphate-sialic acid
GDP	Guanosine diphosphate
GMP	Guanosine monophosphate
GTP	Guanosine triphosphate
GDP-Fuc	Guanosine diphosphate fucose
GDP-Man	Guanosine diphosphate mannose
IP-RP	Ion-pair reverse phase
Trp	Tryptophan
UDP	Uridine diphosphate
UMP	Uridine monophosphate
UTP	Uridine triphosphate
UDP-Gal	Uridine diphosphate galactose
UDP-Glc	Uridine diphosphate glucose
UDP-Hex	Uridine diphosphate hexosamine
UDP-GlcNAc	Uridine diphosphate *N*-acetylglucosamine
UDP-HexNAc	Uridine diphosphate *N*-acetylhexosamine

Disclaimer: This publication reflects the views of Cyrus Agarabi and should not be construed to represent FDA's views or policies.

Electronic supplementary material The online version of this article (https://doi.org/10.1007/s00216-020-02608-6) contains supplementary material, which is available to authorized users.

✉ Seongkyu Yoon
Seongkyu_Yoon@uml.edu

[1] Biomedical Engineering and Biotechnology, University of Massachusetts Lowell, Lowell, MA 01854, USA

[2] Biomedical & Nutritional Sciences, University of Massachusetts Lowell, Lowell, MA 01854, USA

[3] U.S. FDA, CDER/OBP/Division of Biotechnology Review and Research II, Silver Spring, MD 20993, USA

[4] Chemical Engineering, University of Massachusetts Lowell, Lowell, MA 01854, USA

Introduction

N-Linked glycosylation is a cellular process that transfers sugars from glycosyl donors to proteins during protein synthesis [1, 2].

Published online: 16 April 2020

Many therapeutic proteins including monoclonal antibodies (mAbs) are predominantly produced by mammalian cells such as Chinese hamster ovary (CHO) cells and glycosylated following translation. The glycosylation profiles impact a wide range of drug characteristics including stability, efficacy, and safety [3–5]. Nucleotide sugars are a group of glycosyl donors that are important for glycosylation activity [6–9]. There have been a number of mechanistic investigations of the glycosylation donor's effects [1, 6, 10–13] and an increasing interest in interpreting nucleotide sugar metabolism with mathematical models [14–18]. Understanding of the quantitative relationship between nucleotide sugars and glycosylation process will further enhance the quality control of biologics during their production in mammalian cells.

One hurdle in the field is a lack of methods that can sufficiently profile a wide range of common nucleotide sugars, including guanosine diphosphate mannose (GDP-Man), guanosine diphosphate fucose (GDP-Fuc), uridine diphosphate galactose (UDP-Gal), uridine diphosphate glucose (UDP-Glc), uridine diphosphate *N*-acetylglucosamine (UDP-GlcNAc), uridine diphosphate *N*-acetylgalactosamine (UDP-GalNAc), and cytidine monophosphate-sialic acid (CMP-SA).

It is challenging to achieve complete chromatographic separation for all these nucleotide sugars. First, the nucleotide sugar isomers, especially UDP sugars often co-elute due to their similar structure. For instance, the pair of UDP-hex (UDP-Gal and UDP-Glc) differs only by the orientation of a hydroxyl (–OH) group. This similarity is also present with UDP-hexNAc (UDP-GlcNAc and UDP-GalNAc). Second, other compounds such as simple nucleotides and amino acids in cell extracts can co-elute with nucleotide sugars and produce major UV-absorbing peaks. Lastly, the nucleotide sugars or isomers present at low abundance must be well separated from the high-abundance compounds in cell extracts. All these challenges could be met by a high-resolution separation.

Several approaches to this problem have been reported in literature, including ion-pair reverse phase chromatography [19–21], anion-exchange [22], liquid chromatography-mass spectrometry (LC-MS) [6, 23–28], and capillary electrophoresis [29]. Based on the literature data, ion-pair reverse phase (IP-RP) chromatography introducing tetrabutylammonium bisulfate is one of the most powerful separation methods for nucleotide sugars [20, 21, 30, 31]. The shortcoming is that the method is incompatible with mass spectrometry. The best separation in literature was shown in Nakajima's study (2010) using a single high carbon load column [32]. In our preliminary work using the same column and conditions as described in that study, complete separation of the UDP sugar isomer compounds was however not achieved, indicating that the method can be subject to varying results, in different laboratories and chromatographic systems.

In our preliminary work, we had also explored HILIC and normal phase separations, which might have been alternative methods for nucleotide sugars as a group of polar compounds; however, we found these methods were less powerful than IP-RP to separate UDP sugar isomers. Therefore, we extended the technique of IP-RP to achieve a further increase in nucleotide sugar separation as well as method robustness. The strategy applied is based on core-shell particle columns and connections of multiple columns in tandem, as a principle to achieve more theoretical plates in the chromatographic separation. Major nucleotide sugars including UDP sugar isomers are separable by this method. Although the method is incompatible with MS, it is an effective strategy to achieve enhanced separation of nucleotide sugars and thus enable studies of these compounds in the field of mammalian cell culture. The method is currently conducted with conventional HPLC but has the potential to be adapted to a U(H)PLC and sub 2 μm columns in laboratories that have access to these resources.

Methods

Materials

The standards used in the study include tryptophan and 12 nucleotides: adenosine triphosphate (ATP), cytidine triphosphate (CTP), guanosine triphosphate (GTP), uridine triphosphate (UTP), adenosine diphosphate (ADP), cytidine diphosphate (CDP), guanosine diphosphate (GDP), uridine diphosphate (UDP), adenosine monophosphate (AMP), cytidine monophosphate (CMP), guanosine monophosphate (GMP), uridine monophosphate (UMP), and 8 nucleotide sugars including CMP-SA, UDP-Gal, UDP-Glc, GDP-Man, UDP-GalNAc, UDP-GlcNAc, GDP-Fuc, and GDP-Glucose (GDP-Glc), one that does not naturally exist in CHO cells and was used as an internal control. All these compounds were purchased from Sigma-Aldrich (St. Louis, MO). Stock solutions of each standard were prepared and the aliquots were stored at − 20 °C. The standard mixture was made from the individual standard stock solution prior to use. Tetrabutylammonium bisulfate (HPLC grade), 1 M of both potassium phosphate dibasic solution and potassium phosphate monobasic solution, perchloric acid (PCA), potassium hydroxide, and methanol (HPLC grade) were also purchased from Sigma-Aldrich (St. Louis, MO). The PCA was diluted to 0.5 M solution before use.

Cell culture and sampling

A CHO cell line used in the study was derived from CHO-S and produced adalimumab biosimilar. The cell line was kindly provided by our industrial collaborator. A vial of CHO-GS

cells was thawed and seeded in Gibco™ FortiCHO medium (Thermo Fisher Scientific, Waltham, MA). The cell culture was inoculated with 0.5 million/mL of viable cells in 125-mL shake flask in a 30 mL working volume. Cell counts were performed on Cedex HiRes Analyzer (Roche, Basel, Switzerland). A volume of cell culture broth was collected that contained 2-3 million cells, and centrifuged at 1000 rpm for 5 min. After discarding the supernatant, 1 mL of cold PBS was added to wash the pellets by re-suspending the cell pellets. Subsequently, another centrifugation step was conducted at 1000 rpm for 5 min. The PBS was discarded, and the pellets were quickly frozen in dry ice and stored at − 80 °C until extraction.

Extraction of nucleotide sugars

After cell pellets were thawed, 200 μL of 0.5 M PCA was added to disrupt the cell pellets and release the nucleotides. An aliquot of 0.5 μL of 20 mM GDP-Glc standard was spiked (the GDP-Glc is absent in natural extracts and thus added to the cell extract as an internal control). The cell lysate was incubated on ice for 5 min and centrifuged at 2000×*g* for 3 min at 4 °C. The supernatant was transferred to a new Eppendorf tube and kept on ice. Another 200 μL of 0.5 M PCA was then added to the cell pellets in the original tube, followed by a spike of another 0.5 μL of 20 mM GDP-Glc standard. The mixture was incubated on ice for 2 min and centrifuged at 18000×*g* for 3 min at 4 °C. The supernatant was merged with the previous one. To neutralize the solution, an aliquot of 56 μL of 2.5 M potassium hydroxide in 1.1 M dipotassium hydrogenphosphate was added, and the sample was incubated on ice for 2 min. The sample was then centrifuged at 18000×*g* for 1 min to remove potassium perchlorate precipitate. Thereafter, the supernatant was filtered by a 0.22-μm PVDF syringe filter into a clean Eppendorf tube. The sample was stored at 4 °C.

HPLC analysis

The separation and detection for nucleotide sugars were performed on an Agilent 1100 high performance liquid chromatography (HPLC) system paired with a UV-diode array detector (Agilent Technologies, Santa Clara, CA). Buffer A was 0.1 M potassium phosphate with 8 mM tetrabutylammonium phosphate, adjusted to pH 6.5. Buffer B was constituted with 70% mobile A and 30% methanol [20, 21, 30]. Buffer A was purified by 0.22-μm filter prior to use and stored at 4 °C. The HPLC columns used were Kinetex® 2.6 μm 100 × 4.6 mm (Phenomenex, Torrance CA). Columns were connected using short, narrow-diameter tubing. A Kinetex® C18 guard column was installed at the head of the first column. An optimized method using two columns in tandem was run at a flow rate of 0.6 mL/min with the following conditions: 0–16 min, 5% B (isocratic separation of major nucleotide sugars); 16–16.5 min, 100% B; 16.5–30 min, 100% B (removing late-eluting compounds); 30–30.5 min, 5% B; 30.5–45 min (re-conditioning), 5% B; the total run time was 45 min. The wavelength of UV detector was set at 260 nm. The temperature of the column compartment was controlled at 40 °C. The UV spectrum of each peak was collected by the diode array detector. The injection volume was 5 μL if not otherwise indicated. After the analyses, the columns were washed with water to remove salt residues and stored in 30% methanol.

Peak annotation

The retention time for each nucleotide sugar was identified by analysis of standards. The retention time was used to establish the initial identity of peaks in the chromatographic trace of cell extract samples. The peak identities from cell extracts were further confirmed by the unique spectra of adenosine (A), uridine (U), cytidine (C), guanosine (G) compounds, and tryptophan (since the tryptophan also absorbs at 260 nm). The spectra of these compounds are shown in Electronic Supplementary Material (ESM) Fig. S1.

Calculations

The separation parameters calculated in the study include capacity factor (k'), theoretical plates (N), separation factor or selectivity (α), and resolution (Rs). The calculations were carried out by the following equations, where t_R represents retention time, t_0 represents the dead time of the column, and $w_{0.5}$ represents peak width at the half-peak height.

$$k' = \frac{t_R - t_0}{t_0} \tag{1}$$

$$N = 5.54 \left(\frac{t_R}{w_{0.5}}\right)^2 \tag{2}$$

$$\alpha = \frac{k_2'}{k_1'} = \frac{t_{R2} - t_0}{t_{R1} - t_0} \tag{3}$$

$$R_s = \frac{1}{4} \sqrt{N} \left(\frac{\alpha - 1}{\alpha}\right) \left(\frac{k'}{1 + k'}\right) \tag{4}$$

Results

Figure 1 summarizes a work flow for the method described here. First, IR-RP parameters were optimized with single column separation; then, the separation power was increased by connecting columns in tandem. Finally, method efficiency and reproducibility were improved by further modifying the analytical conditions.

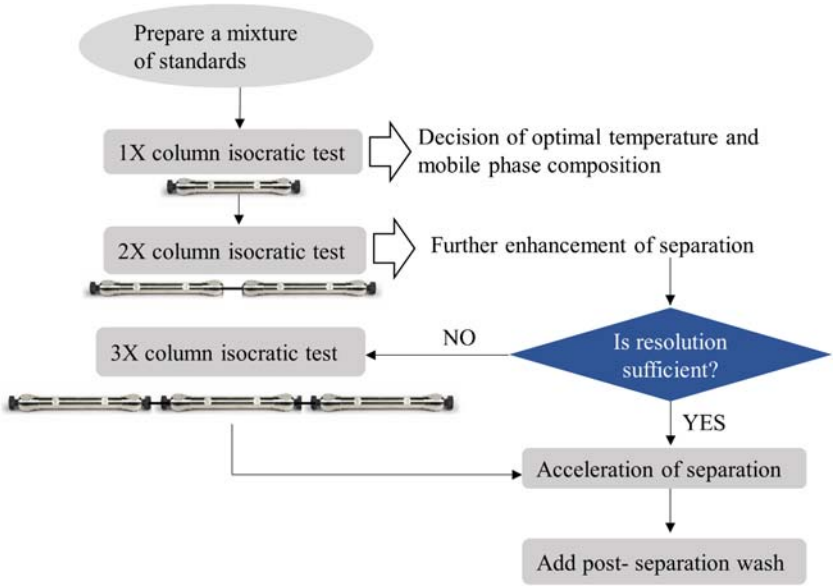

Fig. 1 Workflow of the method development for nucleotide sugar separation

Parameters of IP-RP chromatography

To achieve optimal performance by IP-RP chromatography, the impact of analytical parameters on chromatographic performance were first evaluated using a single core-shell column (shown in Fig. 2). The step was to quickly assess the analytical conditions and decide the optimal conditions for the subsequent tests. A test sample was a standard mixture of CMP-SA, UDP-Gal, UDP-Glc, GDP-Man, UDP-GalNAc, UDP-GlcNAc, GDP-Fuc, GDP-Glc, CDP, and tryptophan. Notably, CDP and tryptophan were added in this mixture because we found them eluting from cell extracts within the range of nucleotide sugars' elution time, while these two compounds also had strong absorptivity at 260 nm.

To distinguish each compound in Fig. 2, every individual standard was run on the column to find out the retention time. The compounds in the mixture were identified by aligning the retention time as well as examining the UV spectrum of each peak, as described in the Methods section.

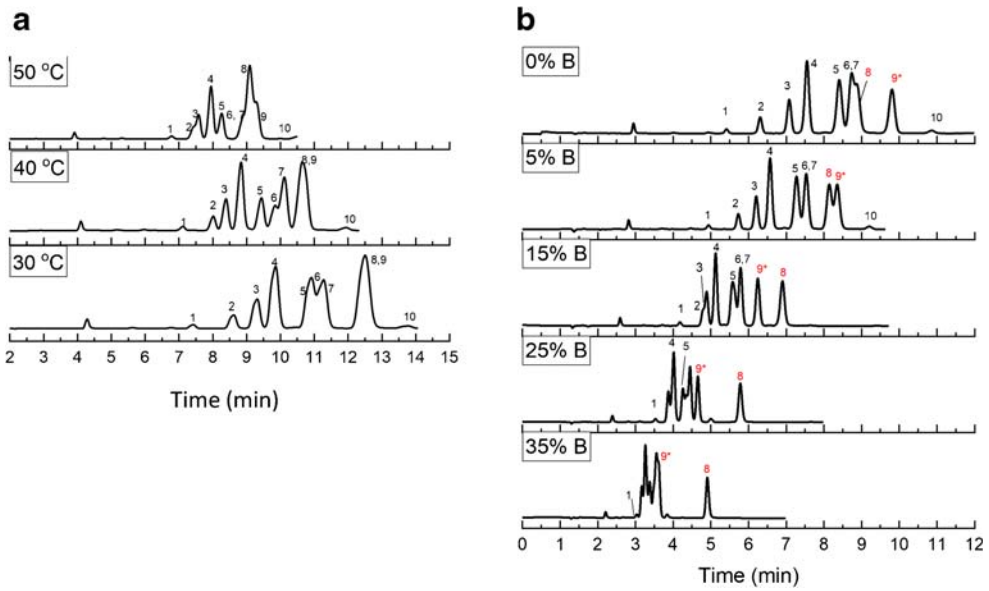

Fig. 2 The impact of analytical parameters on chromatographic separation. **a** Effects of temperature. All the HPLC runs were performed with one column (1×), an isocratic mobile phase combining 95% buffer A and 5% buffer B, and a flow rate of 0.4 mL/min. **b** Effects of mobile phase composition. The composition of isocratic mobile phase B varied between 0 and 35%. All the runs were performed with one column (1×), 40 °C and flow rate 0.6 mL/min. The IDs of compounds in the chromatograms are labeled numerically as follows: (1) CMP-Sialic acid; (2) CDP; (3) UDP-Gal; (4) UDP-Glc; (5) GDP-Man; (6) UDP-GalNAc; (7) UDP-GlcNAc; (8) Trp; (9) GDP-Glc*, and (10) GDP-Fuc

For example, the UV spectrum of tryptophan is distinct from any of the nucleotide compounds (ESM Fig. S1).

The first test examined the impacts of temperature on the separation. The mixture of standards was separated on a single column respectively at 30 °C, 40 °C, and 50 °C. All the tests were run at an isocratic condition containing 5% buffer B and a flow rate of 0.4 mL/min. As shown in Fig. 2a, the separation of compounds in the mixture compounds was significantly affected by the temperature. As the temperature increased, the exchange rate of analytes between the mobile and stationary phases increases, resulting in shortened retention time. Correspondingly, the resolution for the mixture of compounds was decreased. As a result, 40 °C was determined to be reasonable for both the separation outcomes and the time required for elution.

In the next test, the standards were separated isocratically at different ratios between buffers A and B. The different conditions tested contained 0%, 5%, 15%, 25%, and 35% of buffer B. This gradient of ratios represented an increasing composition of methanol in the mobile phase. All the runs used a flow rate of 0.6 mL/min and 40 °C. As shown in Fig. 2b, a lower percentage of buffer B provided a better separation and a longer elution time of nucleotide sugars.

As the retention for all the compounds decreased with the addition of buffer B, it was noted that the decrease was faster for the nucleotide sugars than the amino acid tryptophan. Interestingly, the order of tryptophan (peak #8) and GDP-Glc (peak #9*) switched as the percentage of buffer B increased in the mobile phase (Fig. 2b): the peak of tryptophan showed up earlier than GDP-Glc with low percentage of buffer B, but shifted to the back of the GDP-Glc with increased percentage of buffer B. The distance between these two compounds was increased with the addition of buffer B. The phenomenon indicated a differential impact on the tryptophan and the nucleotide sugars by the change in the mobile phase composition, which will be discussed later in the mechanism of the IP-RP method.

Nucleotide sugar separation using multiple columns in tandem

The data from the above experiments indicated that, the optimal temperature was 40 °C and the mobile phase was 95% A and 5% B. With these conditions, the ability to separate the same mixture of standards was tested with two or three columns connected in tandem (respectively referred as 2× and 3×). As shown in Fig. 3a, the separation was continuously improved as more columns were used. With 1× column, there was little separation between UDP-GalNAc, UDP-GlcNAc, and tryptophan (peak #6, 7, and 8). With 2× columns, those compounds were completely separated. With 3× columns, the distance between these compounds was further expanded.

To understand how the multiple columns in tandem have improved the separation resolution, we calculated the theoretical plates (N), capacity factor (k'), and selectivity (α) affected by the number of columns in tandem, using Eqs. (1)–(4) shown in the Methods section. These four factors collectively determine the separation resolution (Rs). As shown in Fig. 3b, the number of theoretical plates (N) increased with the number of columns connected, reaching approximately 20,000, 40,000, and 60,000 theoretical plates with the 1×, 2×, and 3× columns. On the other hand, the capacity factor (k') and selectivity (α) remain unchanged. Therefore, the increase of the theoretical plate number was the main reason for the improved resolution (Rs).

The impact of the mobile phase flow rate on the chromatographic separation was then evaluated using two columns connected (2×) at flow rates of 0.4, 0.6, and 0.8 mL/min. The maximum backpressure during a run did not exceed 400 bars. The results (Fig. 4) showed that the separation resolution remained satisfactory at both of 0.4 and 0.6 mL/min, but decreased at a higher flow rate 0.8 mL/min.

Separation of nucleotide sugars in cell extracts

Then, we evaluated the separation with nucleotide sugars prepared from cell extracts, comparing the analytical conditions described above. The sample was an extract from 2.8 million CHO cells, spiked with GDP-Glc and injected at 5 μL volume. Three HPLC tests were run respectively using 1×, 2×, and 3× columns. Because of considerations of column pressure, the flow rate was 0.8 mL/min for 1×, 0.6 mL/min for 2×, and 0.4 mL/min for 3×. As shown in Fig. 5, the separation was improved by the addition of more columns in tandem. Specifically, the peaks between UDP-GlcNAc, tryptophan, and GDP-Glc (peak #6, 7, and 8) were unable to be resolved within the 1× column. The employment of 2× columns successfully resolved the peaks #6, 7, and 8; the only unsolved nucleotide sugar was CMP-SA which was overlapped by an adjacent big peak (RT 10 min). By further use of 3× columns, the CMP-SA in cell extracts became also separated. Notably, CMP-SA, GDP-Man, and GDP-Fuc were less abundant than other nucleotide sugar components, and measurement of these compounds required excellent chromatographic separation.

Column variability

Since the method involves the usage of multiple columns, the variability of single columns was tested. In the test, four columns from different manufacturing lots (including the ones used in the above studies) were tested individually using a cell extract sample. The results are shown in ESM Fig. S2. The overall separation pattern was comparable. However, the

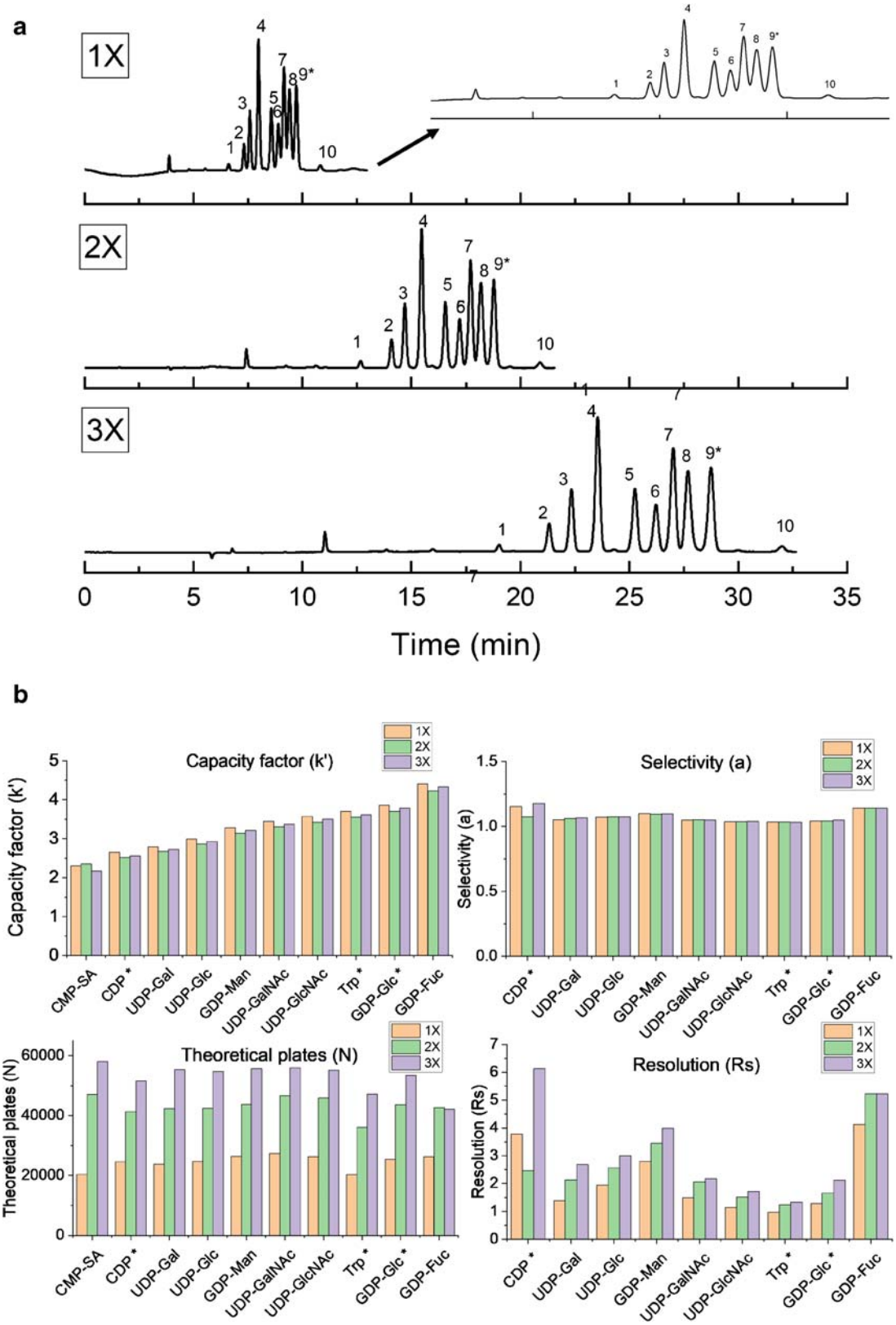

Fig. 3 Separation of mixture standards from 1×, 2×, and 3× columns. **a** Chromatograms generated using 1×, 2×, and 3× columns. All the HPLC runs were performed isocratically with mobile phase combining 95% buffer A and 5% buffer B, at 40 °C and flow rate 0.4 mL/min. The IDs of compounds in the chromatograms are labeled numerically as follows: (1) CMP-Sialic acid; (2) CDP; (3) UDP-Gal; (4) UDP-Glc; (5) GDP-Man; (6) UDP-GalNAc; (7) UDP-GlcNAc; (8) Trp; (9) GDP-Glc*, and (10) GDP-Fuc. **b** The calculation of theoretical plates (*N*), capacity factor (*k'*), selectivity (α), and resolution (*R*s) using 1×, 2×, and 3× columns

resolution for the closely eluting compounds showed some variability (as shown in the red boxes in ESM Fig. S2).

Post-isocratic separation

After the nucleotide sugars were resolved isocratically, more highly-retained compounds like nucleotide triphosphates were still held on the stationary phase and needed to be removed to avoid contamination in following HPLC runs. To evaluate the retention of all the compounds in the cell extracts, a sample prepared from cells was analyzed with one column, using the initial isocratic conditions, until all the compounds were eluted (Fig. 6a). Two late-eluting compounds ADP and ATP were found abundant in the cell extract. ATP was the last peak and took 8.3 times longer to elute than GDP-Glc to elute (retention time, 55 min for ATP versus 6.6 min for GDP-Glc). To accelerate the removal of ADP and ATP, we modified the method by adding a stringent wash using 100% B after the elution of peaks of interest, which eluted ATP after five mobile phase column volumes (Fig. 6b). After the rinse, we equilibrated the columns by five further column volumes of the initial mobile phase. Runs following this wash cycle were found to be free of carryover and the traces were consistent between consecutive runs. The cycle was similarly adapted to 2× columns.

Linearity and reproducibility

The linearity of the method was tested using 2× columns by injecting a standard mixture with a series of volumes. As shown in Fig. 7, the chromatographic peak area and the amount of nucleotide sugar injected (from 1 to 100 pmol) showed a linear relationship. The baseline noise from a blank run was under 0.1 mAu.

To test the reproducibility of the method, the same volume of mixture standard was injected for a total of 8 times across different days. The tests used 2× columns and were conducted at the optimal conditions of the study. The variation of the retention time and peak area of each compound are reported in Table 1.

Five aliquots of 2.8 million cells were extracted in parallel to examine the variability resulting from the cell extraction steps. At each extraction, the internal control of GDP-Glc was spiked into the sample. Each extracted sample was tested using the HPLC method with 2× columns. The peak area obtained for each compound are shown in Table 2. The peak area of each peak was normalized to the peak area of GDP-Glc.

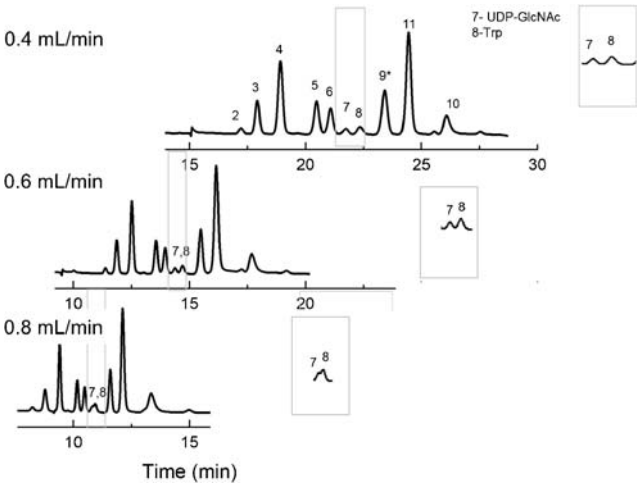

Fig. 4 Tests of chromatographic separation using different flow rates. All the HPLC runs were performed with two columns (2×), isocratic mobile phase combined with 95% buffer A and 5% buffer B, and at 40 °C. The IDs of compounds in the chromatograms are labeled numerically as follows: (1) CMP-Sialic acid; (2) CDP; (3) UDP-Gal; (4) UDP-Glc; (5) GDP-Man; (6) UDP-GalNAc; (7) UDP-GlcNAc; (8) Trp; (9) GDP-Glc*, (10) GDP-Fuc, and (11) UDP

Discussion

About using multiple columns in tandem

Enhanced resolution and selectivity are needed to profile the complex nucleotide sugar mixtures found in cell extracts. The conventional approach with a single analytical column, and a length between 5 and 25 cm inevitably reach a ceiling of separation. In this work, improved chromatographic separation was achieved by using core-shell columns and connecting multiple columns in tandem, which enabled a high number of theoretical plates. Use of multiple columns in series could theoretically raise a concern about peak broadening and loss of resolution. However, our study proves that connecting columns has continuously improved the separation resolution, and provided an increasing number of theoretical plates. Core-shell stationary phase technology has been reported to generate a better separation efficiency than columns with porous stationary phase [33]. A Kinetex® C18 column is typically specified with 264,600 plates/meter by the manufacturer. As expected, our work has empirically observed 400,000–500,000 plates/meter by connecting two columns. We found that two coupled columns can provide enough power to separate the majority of the nucleotide sugars in CHO cells, including UDP sugar isomers, while three coupled columns can completely resolve all the seven nucleotide sugars in the cell extracts.

One drawback of this strategy is that HPLC run time increases with the number of columns. Therefore, there is a tradeoff between separation resolution and analysis time. Increased flow rate can be potentially used to reduce the method run time; however, the speed could be limited by the pressure limits of the liquid chromatographic system, for which the highest backpressure occurs during the method when the

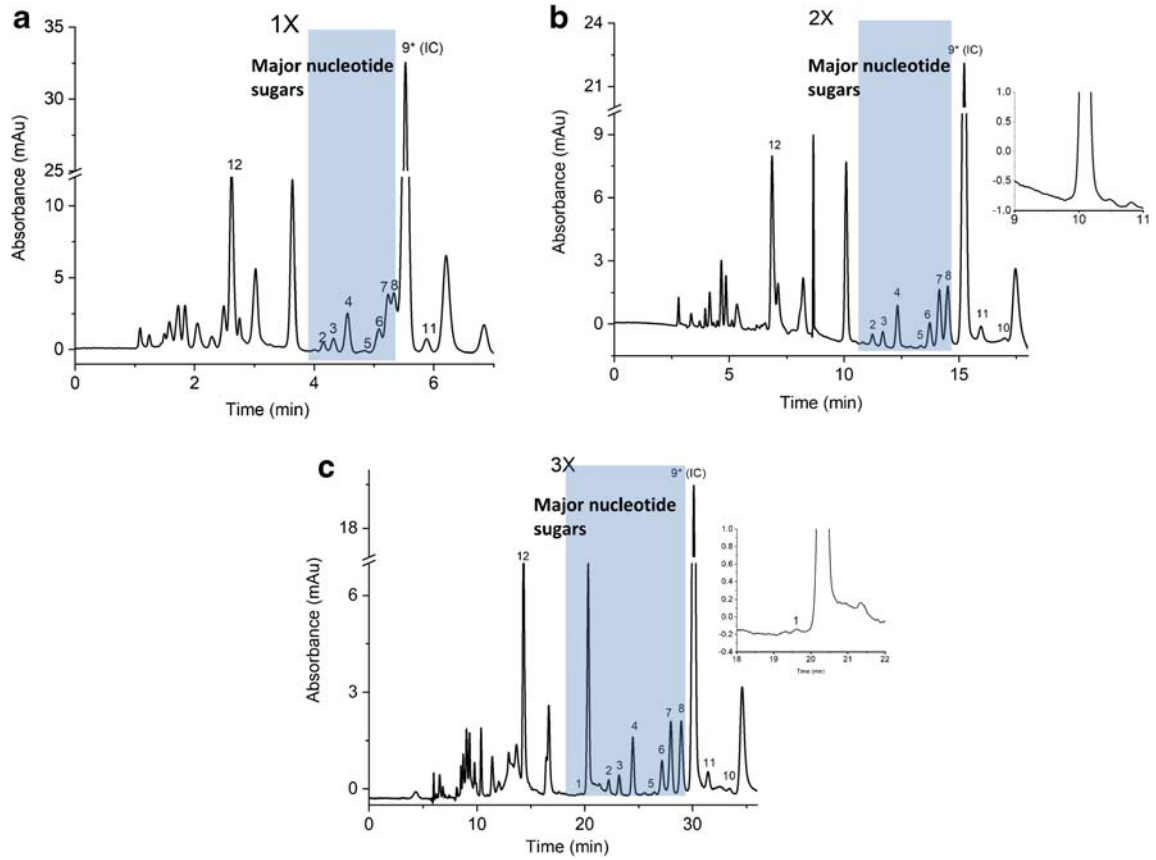

Fig. 5 Separation of nucleotide sugars from cell extracts using 1× (**a**), 2× (**b**), and 3× (**c**) columns. All the HPLC runs were performed with mobile phase containing 95% buffer A and 5% buffer B, at 40 °C. Flow rates were respectively 0.8 mL/min for 1×, 0.6 ml/min for 2×, and 0.4 mL/min for 3×. The IDs of compounds in the chromatograms are labeled numerically as follows: (1) CMP-Sialic acid; (2) CDP; (3) UDP-Gal; (4) UDP-Glc; (5) GDP-Man; (6) UDP-GalNAc; (7) UDP-GlcNAc; (8) Trp; (9) GDP-Glc*; (10) GDP-Fuc; (11) UDP, and (12) GMP

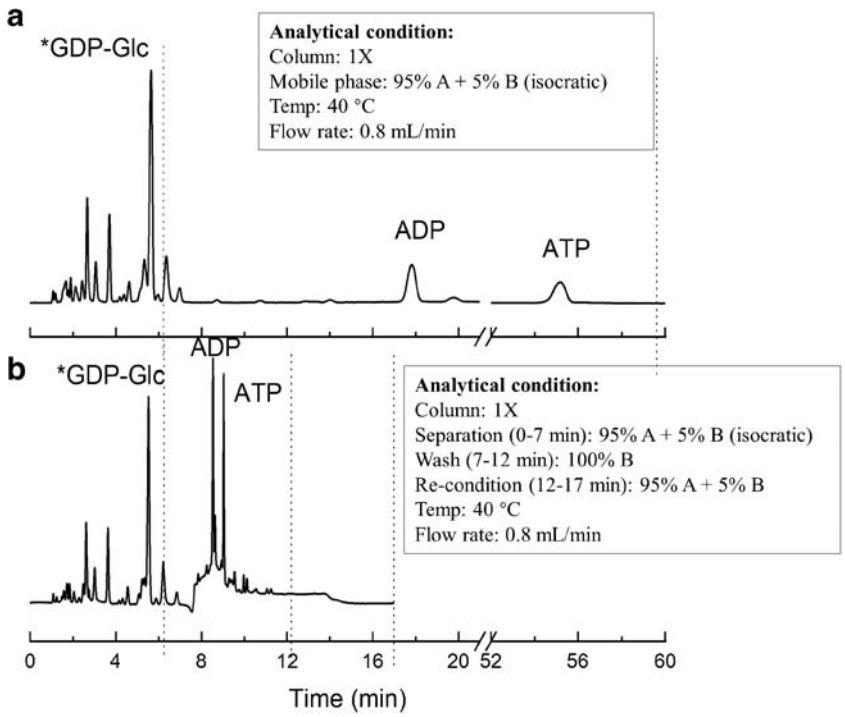

Fig. 6 A complete run including a wash step after isocratic separation. **a** Analysis of cell extract maintained at the isocratic condition (5% B). **b** Analysis starting at 5% B, followed by a wash using 100% B, and re-equilibration by 5% B

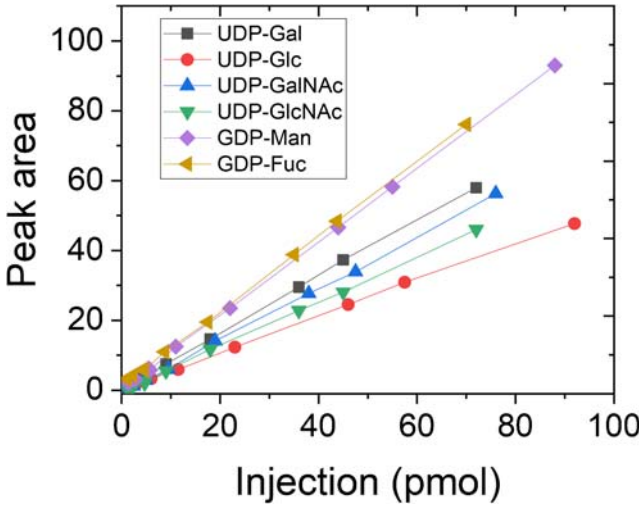

Fig. 7 Method linearity tested with 2× columns and nucleotide sugar standards

columns are rinsed using 100% buffer B. The flow rates can impact the separation efficiency, depending on column packing, particle size, and others. In this work, a reasonable flow rate was 0.6 mL/min when using two columns connected and required 45 min total run time, including re-equilibration. A better balance between the separation resolution and run time may be obtained by using ultra-performance liquid chromatography (UPLC) system, which have higher pressure limits, while the best flow rate in the regime of UPLC needs to be evaluated.

As shown in our work, single columns would result in variability of separation resolution. Therefore, the performance of the separation can be subject to column variations from different manufacturing lots (or column usage conditions) and different systems. In this work, such possible variability was less problematic because the resolving power was improved by connecting multiple columns. It will thus be practical to apply this method across different laboratories and analytical systems to achieve satisfactory results regardless of the variations that exist between individual columns.

Table 1 Multi-injection reproducibility ($n = 8$) from different days

Compounds	Retention time			Peak area		
	Mean	SD	CV%	Mean	SD	CV%
UDP-Gal	10.990	0.795	7.237	98.263	5.786	5.888
UDP-Glc	11.754	0.666	5.669	228.888	13.197	5.766
GDP-Man	13.068	0.386	2.954	104.500	6.106	5.843
UDP-GalNAc	13.586	0.264	1.945	81.188	8.479	10.443
UDP-GlcNAc	14.197	0.211	1.487	14.840	2.805	18.904
GDP-Fuc	17.230	0.259	1.502	6.963	0.940	13.494
GDP-Glc*	15.437	0.197	1.278	168.313	10.530	6.256

Table 2 Reproducibility of cell extractions ($n = 5$)

Compounds	Peak area (normalized to GDP-Glc*)		
	Average	SD	CV%
UDP-Gal	0.0216	0.0014	6.3622
UDP-Glc	0.0715	0.0003	0.3846
GDP-Man	0.0020	0.0003	13.5238
UDP-GalNAc	0.0327	0.0015	4.4742
UDP-GlcNAc	0.0773	0.0100	12.8691
GDP-Fuc	0.0041	0.0003	7.6218

*Peak area of compounds/peak area of GDP-Glc

About the mechanisms of IP-RP

IP-RP chromatography is considered to be a method that used mixed separation mechanisms. A proposed mechanism, that would explain the increased retention of nucleotide sugars with multiple negatively-charged phosphate groups, is that the ion-pair reagent initially forms a coating on the stationary phase and creates a charged surface where analytes are captured via the attraction between counter ions. A theory in detail is proposed in Fig. 8 to explain the chromatographic behavior throughout a method cycle and accounts for the difference in the retention time of molecules responding to different weights of buffer B that have been shown in Fig. 2b.

At the equilibration stage, ion-pair reagent (tetrabutylammonium) is attracted by the C18 stationary phase via the hydrophobic interaction and forms a layer near the stationary phase. The new surface is both hydrophobic and charged by the presence of N+ cation from the tetrabutylammonium. When cell extracts are applied, molecules in the samples are attracted to the stationary phase via two different modes of interactions: counter-ion absorption and hydrophobic interaction. Nucleotide sugars are molecules with negative charge on phosphate(s), and their charge strength is dependent on the number of phosphates contained. Once entering the columns (Fig. 8a), nucleotide sugars are temporarily absorbed on the stationary phase by the attraction of N+ cation near the stationary surface. There is an increase in retention time with the compounds that have more phosphates. In contrast, the tryptophan is a neutral molecule and has no interaction with the charge near the stationary surface; however, tryptophan is a hydrophobic molecule and is attracted to the stationary phase by the hydrophobic interaction.

When the composition of buffer B increases in the mobile phase, this can cause multi-dimensional effects on the retention of nucleotide sugars and tryptophan. First, the fraction of ion-pair reagent coated on the stationary phase is reduced and the stationary phase becomes less charged; this causes a

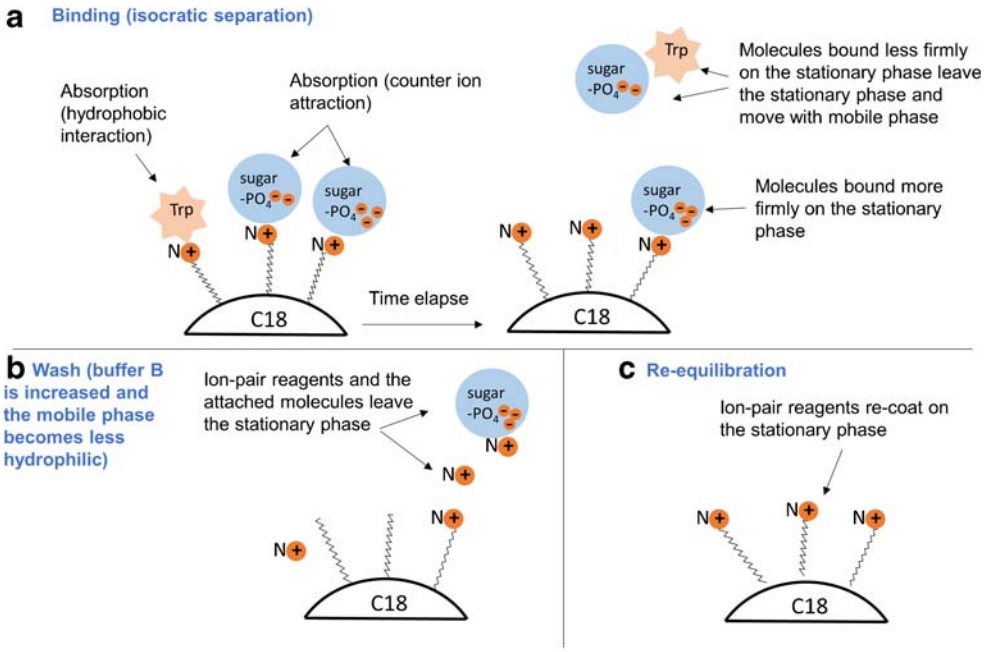

Fig. 8 Hypothetical theory of the chromatographic behavior during a cycle of the method. **a** Isocratic separation. **b** Wash stage. **c** Re-equilibration

general reduction of the affinity of nucleotide sugars. Second, the solvent becomes more hydrophobic; this results in an increasing competition from the mobile phase with the stationary phase for tryptophan. Because of these simultaneous but distinct effects, the rates of retention change occurring with nucleotide sugars and tryptophan appeared to be different, as the scenario shown in Fig. 2b.

At the wash stage (Fig. 8b), the mobile phase containing 100% buffer B becomes very hydrophobic; thus, part of the ion-pair reagents tetrabutylammonium along with highly absorbed phosphate ions is eluted from the stationary phase. By re-equilibration (Fig. 8c), the tetrabutylammonium is re-coated onto the surface of the stationary phase.

The study reveals that temperature and mobile phase composition are two critical parameters that can significantly change the behavior of the chromatographic separation. HPLC conditions must be equilibrated sufficiently with the initial mobile phase (containing 95% A and 5% B) to maintain consistency across runs. Previous studies suggested a need for long equilibration for IP-RP chromatography [34]. In this study, five column volumes of the initial mobile phase were found sufficient for satisfactory consistency in consecutive runs. The column temperature should be tightly controlled for run to run consistency.

Conclusion

We have proposed and comprehensively investigated an approach of using core-shell columns and multiple columns in tandem to achieve enhanced chromatographic separation for nucleotide sugars, especially UDP sugar isomers. Key parameters affecting chromatographic results were identified and a workflow strategy is described to tune the optimal analysis method. We anticipate that this method can help expedite the studies in the biopharmaceutical process and other biological fields where there is increasing knowledge of nucleotide sugar metabolism [35].

Acknowledgments The authors gratefully thank Dr. Maurizio Cattaneo for providing the cell line and Dr. Kurt Brorson for the support of this study.

Funding information The study was supported by grants from NSF (1706731) and NSF/IUCRC AMBIC (1624718).

Compliance with ethical standards

Conflict of interest The authors declare that they have no conflict of interest.

Disclaimer This publication reflects the views of the author and should not be construed to represent FDA's views or policies.

References

1. Sha S, Agarabi C, Brorson K, Lee DY, Yoon S. N-Glycosylation design and control of therapeutic monoclonal antibodies. Trends Biotechnol. 2016;34(10):835–46.
2. Lalonde ME, Durocher Y. Therapeutic glycoprotein production in mammalian cells. J Biotechnol. 2017;251:128–40.
3. Higel F, Seidl A, Sorgel F, Friess W. N-glycosylation heterogeneity and the influence on structure, function and pharmacokinetics of monoclonal antibodies and Fc fusion proteins. Eur J Pharm Biopharm. 2016;100:94–100.
4. Wang Q, Chung CY, Yang W, Yang G, Chough S, Chen Y, et al. Combining butyrated ManNAc with glycoengineered CHO cells

improves EPO glycan quality and production. Biotechnol J. 2019;14(4):e1800186.
5. Wang Q, Yang G, Wang T, Yang W, Betenbaugh MJ, Zhang H. Characterization of intact glycopeptides reveals the impact of culture media on site-specific glycosylation of EPO-Fc fusion protein generated by CHO-GS cells. Biotechnol Bioeng. 2019;116(9): 2303–15.
6. Villiger TK, Steinhoff RF, Ivarsson M, Solacroup T, Stettler M, Broly H, et al. High-throughput profiling of nucleotides and nucleotide sugars to evaluate their impact on antibody N-glycosylation. J Biotechnol. 2016;229:3–12.
7. Blondeel EJ, Braasch K, McGill T, Chang D, Engel C, Spearman M, et al. Tuning a MAb glycan profile in cell culture: supplementing N-acetylglucosamine to favour G0 glycans without compromising productivity and cell growth. J Biotechnol. 2015;214:105–12.
8. Jedrzejewski PM, del Val IJ, Constantinou A, Dell A, Haslam SM, Polizzi KM, et al. Towards controlling the glycoform: a model framework linking extracellular metabolites to antibody glycosylation. Int J Mol Sci. 2014;15(3):4492–522.
9. Kochanowski N, Blanchard F, Cacan R, Chirat F, Guedon E, Marc A, et al. Influence of intracellular nucleotide and nucleotide sugar contents on recombinant interferon-gamma glycosylation during batch and fed-batch cultures of CHO cells. Biotechnol Bioeng. 2008;100(4):721–33.
10. Wong NS, Wati L, Nissom PM, Feng HT, Lee MM, Yap MG. An investigation of intracellular glycosylation activities in CHO cells: effects of nucleotide sugar precursor feeding. Biotechnol Bioeng. 2010;107(2):321–36.
11. Sumit M, Dolatshahi S, Chu AA, Cote K, Scarcelli JJ, Marshall JK, et al. Dissecting N-glycosylation dynamics in Chinese hamster ovary cells fed-batch cultures using time course omics analyses. iScience. 2019;12:102–20.
12. Naik HM, Majewska NI, Betenbaugh MJ. Impact of nucleotide sugar metabolism on protein N-glycosylation in Chinese hamster ovary (CHO) cell culture. Curr Opin Chem Eng. 2018;22:167–76.
13. Sha S, Yoon S. An investigation of nucleotide sugar dynamics under the galactose supplementation in CHO cell culture. Process Biochem. 2019;81:165–74.
14. Jimenez del Val I, Nagy JM, Kontoravdi C. A dynamic mathematical model for monoclonal antibody N-linked glycosylation and nucleotide sugar donor transport within a maturing Golgi apparatus. Biotechnol Prog. 2011;27(6):1730–43.
15. Del Val IJ, Polizzi KM, Kontoravdi C. A theoretical estimate for nucleotide sugar demand towards Chinese hamster ovary cellular glycosylation. Sci Rep. 2016;6:28547.
16. Sha S, Huang Z, Agarabi C, Lute S, Brorson K, Yoon S. Prediction of N-linked glycoform profiles of monoclonal antibody with extracellular metabolites and two-step intracellular models. Processes. 2019;7(4):227.
17. Burleigh SC, van de Laar T, Stroop CJM, van Grunsven WMJ, O'Donoghue N, Rudd PM, et al. Synergizing metabolic flux analysis and nucleotide sugar metabolism to understand the control of glycosylation of recombinant protein in CHO cells. BMC Biotechnol. 2011;11(1):95.
18. Sha S, Huang Z, Wang Z, Yoon S. Mechanistic modeling and applications for CHO cell culture development and production. Curr Opin Chem Eng. 2018;22:54–61.
19. Räbinä J, Mäki M, Savilahti EM, Järvinen N, Penttilä L, Renkonen R. Analysis of nucleotide sugars from cell lysates by ion-pair solid-phase extraction and reversed-phase high-performance liquid chromatography. Glycoconj J. 2001;18(10):799–805.
20. Nakajima K, Taniguchi N. Simultaneous quantification of nucleotide sugar metabolism by LC and LC-MS. In: Taniguchi N, et al., editors. Glycoscience: biology and medicine. Tokyo: Springer Japan; 2015. p. 103–10.
21. Kochanowski N, Blanchard F, Cacan R, Chirat F, Guedon E, Marc A, et al. Intracellular nucleotide and nucleotide sugar contents of cultured CHO cells determined by a fast, sensitive, and high-resolution ion-pair RP-HPLC. Anal Biochem. 2006;348(2):243–51.
22. del Val IJ, Kyriakopoulos S, Polizzi KM, Kontoravdi C. An optimized method for extraction and quantification of nucleotides and nucleotide sugars from mammalian cells. Anal Biochem. 2013;443(2):172–80.
23. Jorge TF, Florêncio MH, Ribeiro-Barros AI, António C. Quantification and structural characterization of raffinose family oligosaccharides in Casuarina glauca plant tissues by porous graphitic carbon electrospray quadrupole ion trap mass spectrometry. Int J Mass Spectrom. 2017;413:127–34.
24. Warth B, Siegwart G, Lemmens M, Krska R, Adam G, Schuhmacher R. Hydrophilic interaction liquid chromatography coupled with tandem mass spectrometry for the quantification of uridine diphosphate-glucose, uridine diphosphate-glucuronic acid, deoxynivalenol and its glucoside: in-house validation and application to wheat. J Chromatogr A. 2015;1423:183–9.
25. Eastwood H, Xia F, Lo MC, Zhou J, Jordan JB, McCarter J, et al. Development of a nucleotide sugar purification method using a mixed mode column & mass spectrometry detection. J Pharm Biomed Anal. 2015;115:402–9.
26. Ito J, Herter T, Baidoo EE, Lao J, Vega-Sanchez ME, Michelle Smith-Moritz A, et al. Analysis of plant nucleotide sugars by hydrophilic interaction liquid chromatography and tandem mass spectrometry. Anal Biochem. 2014;448:14–22.
27. Pabst M, Grass J, Fischl R, Léonard R, Jin C, Hinterkörner G, et al. Nucleotide and nucleotide sugar analysis by liquid chromatography-electrospray ionization-mass spectrometry on surface-conditioned porous graphitic carbon. Anal Chem. 2010;82(23):9782–8.
28. Wang T, Chen X, Li L, Cao Y, Zhao L, Chai Y, et al. Characterization of nucleotides and nucleotide sugars in Candida albicans by high performance liquid chromatography–mass spectrometry with a porous graphite carbon column. Anal Lett. 2014;47(2):234–49.
29. Feng HT, Wong N, Wee S, Lee MM. Simultaneous determination of 19 intracellular nucleotides and nucleotide sugars in Chinese hamster ovary cells by capillary electrophoresis. J Chromatogr B Analyt Technol Biomed Life Sci. 2008;870(1):131–4.
30. Ryll T, Wagner R. Improved ion-pair high-performance liquid chromatographic method for the quantification of a wide variety of nucleotides and sugar-nucleotides in animal cells. J Chromatogr B Biomed Sci Appl. 1991;570(1):77–88.
31. St Amand MM, Radhakrishnan D, Robinson AS, Ogunnaike BA. Identification of manipulated variables for a glycosylation control strategy. Biotechnol Bioeng. 2014;111(10):1957–70.
32. Nakajima K, Kitazume S, Angata T, Fujinawa R, Ohtsubo K, Miyoshi E, et al. Simultaneous determination of nucleotide sugars with ion-pair reversed-phase HPLC. Glycobiology. 2010;20(7): 865–71.
33. Fekete S, Ganzler K, Fekete J. Efficiency of the new sub-2 mum core-shell (Kinetex) column in practice, applied for small and large molecule separation. J Pharm Biomed Anal. 2011;54(3):482–90.
34. Zhang J, Raglione T, Wang Q, Kleintop B, Tomasella F, Liang X. Regeneration of tetrabutylammonium ion-pairing reagent distribution in a gradient elution of reversed phase ion-pair chromatography. J Chromatogr Sci. 2011;49:825–31.
35. Lazarowski ER, Shea DA, Boucher RC, Harden TK. Release of cellular UDP-glucose as a potential extracellular signaling molecule. Mol Pharmacol. 2003;63(5):1190–7.